THERMAL PROPERTIES OF ORTHOTROPIC MATERIALS: EXPERIMENTAL STUDY AND CORRELATION WITH MICROSTRUCTURE

M. Thomas, N. Boyard, L. Perez, Y. Jarny and D. Delaunay

Université de Nantes, Nantes Atlantique Universités, CNRS, Laboratoire de Thermocinétique de Nantes, rue Christian Pauc, BP 50609, 44306 Nantes cedex 3, France.
nicolas.boyard@univ-nantes.fr

ABSTRACT

The knowledge of thermal properties of orthotropic layered composite materials and the control of uncertainties associated to their experimental measurements is very important to perform accurate and reliable numerical computations on aircraft structures. In this study, a new experimental design, which has the advantage of estimating simultaneously the three components of the thermal conductivity tensor and the specific heat of orthotropic materials is presented. The parameters estimation is performed by solving a 3-D inverse heat conduction problem. Experimental measurements are made on PMMA samples to validate the methodology and unidirectional carbon fibres reinforced polymer (CFRP) samples.

A complementary approach to experimental measurements is to use predictive models and more especially numerical computations to estimate effective properties (homogenisation process). These latter, based on Finite Elements (FE), develop strongly because the influence of the geometry and spatial distribution of the phases can be accurately taken into account. Nevertheless, calculations have to be performed on a representative volume element (RVE). Effective thermal conductivities, quantitative characterization of unidirectional CFRP microstructure and associated RVE are presented in this contribution.

1. INTRODUCTION

Thermal analyses of composite materials using numerical tools are essential to assess to allowable materials and to predict thermal stresses. The prediction quality of these tools requires the knowledge of input parameters with enough accuracy. The thermo-physical properties of materials used in aeronautic structures make parts of the important and influent parameters. The knowledge of the thermal properties (thermal conductivity tensor and specific heat) of composite materials supposed to be homogenised at the considered scale, as well as the uncertainties associated to their measurements are therefore essential. Even if no standard currently exists to measure the thermal properties, a lot of experimental methods [1-3] enable to characterize orthotropic composite materials. To measure the thermal conductivities along the three main directions and the specific heat, it is necessary to combine or repeat one or several previous methods for an extensive and full thermal characterization.

In the same way, numerical computations based on actual composites microstructure are made to predict effective thermal properties. They are based on F E method, which is adequate tool for this kind of calculation. Fibres spatial distribution as well as phases properties and the associated contrast have a strong impact on thermal and mechanical material performances. This concept is well developed in numerous publications [4-6]. Concerning the thermal field, only few authors [7-8] implement calculations of thermal conductivities (and other properties) based on actual microstructure. The characterization of the microstructure is therefore a crucial point of interest for CFRP composites. Relevant spatial descriptors are then investigated to describe the fibres distribution. All of them can also be used to determine the representative volume

element (RVE). It has to be determined before any calculation if we want to achieve to reliable results.
The first part of this paper aims to present the measurement technique for the simultaneous estimation of all thermal conductivity tensor components and C_p. The estimation strategy and the technical solutions are presented. First experimental results show a good agreement with literature values. In a second part, we investigate the microstructure of unidirectional (UD) composite using image processing techniques and stereological spatial descriptors. We finally determine the RVEs of this microstructure from spatial descriptors as well as effective thermal conductivities ($\lambda^{eff}_{x,y}$) from fibres arrangements.

2. ESTIMATION OF THE THERMAL CONDUCTIVITY TENSOR

2.1. Nomenclature

Cp	Specific heat, $J.kg^{-1}.K^{-1}$
T	Temperature, *K*
X(β)	Sensitivity to β
e	Thickness, *m*
m	Size of β
r	Radius, *m*
t	Time, *s*
Subscripts	
X,Y,Z	Main directions of the composite
x,y,z	Heater reference directions
i=1,2	*1*: heater, *2*: composite

Greek symbols	
β	Unknown parameter vector
φ	Heat flux density, $W.m^{-2}$
Λ	Thermal conductivity tensor
λ	Thermal conductivity component, $W.m.K^{-1}$
ρ	Density, $kg.m^{-3}$

2.2. Experimental device

The experimental device (Figure 1) consists in a thin electrical heater, sandwiched between two similar composite samples. The assembly (heater and samples) is placed in a thermo-regulated vacuum chamber. The vacuum chamber is equipped with a ZnSn window through which the pyrometer measures the surface temperature of the sample.

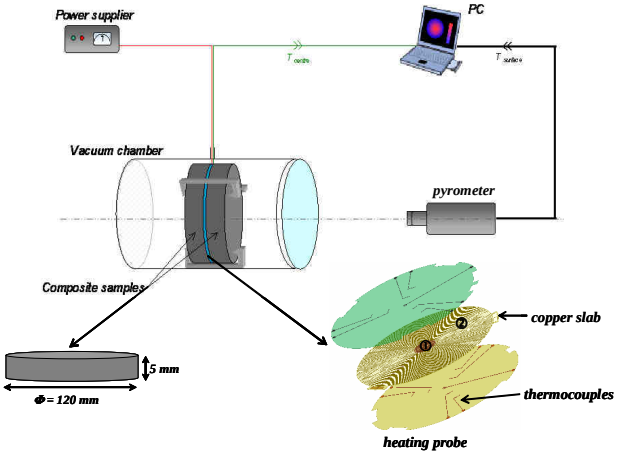

Figure 1: Experimental device

The heater is composed of a stack of Kapton® discs on which are set two distinct circular heating tracks: a central heating disc of radius r_{int}, and a peripheral heating corona between the interior radius r_{int} and the exterior radius r_{max}. Seven micro-thermocouples are located inside the heater. They measure the temperature evolutions

in different directions (for different angles) and at different distances (different radii) from the centre. An IR pyrometer focused on the centre of the upper face of one sample ensures the measurement of the transverse thermal gradient (direction *Oz*). Thin rubber sheets are placed between the composite samples and the heater to limit the roughness effect, and thus to ensure a good interface thermal contact.
The experiment consists in dissipating a known heat flux in the heater and then measuring the resulting thermal rises. The analysis of the temperature evolution in the heater as well as on the sample (diameter: 120mm) upper face permits to characterize the thermal properties of the tested composite material. The measurement temperature range starts from the ambient up to 200°C (maximum temperature for the heater). It is also important to notice that this measurement method was designed to facilitate fast experiments and to prevent composite samples from tedious intrusive instrumentation.

2.3. Identification method

The aim of the developed identification process is to determine the thermal properties of an orthotropic composite material. The set of unknown parameters to be determined, involves the specific heat and the thermal conductivity tensor. The thermal conductivity tensor of an orthotropic material in the coordinate system of the main directions (*OX*, *OY*, *OZ*) is diagonal. The main directions are supposed to be orthogonal. We naturally consider the transverse direction (*OZ*), which is the thickness direction of the sample, as one of the main direction. Concerning the two other main directions, (*OX*) and (*OY*), we decided to name (*OX*) the direction in which the planar thermal conductivity is the most important, and thus (*OY*) the orthogonal direction to the two first ones. However, before any experiments, we do not know the main directions of the composite sample; so we have to determine them. Let us consider the coordinate system of the heater (*Ox*, *Oy*, *Oz*). This system is similar to the composite sample one, but rotated about the (*OZ*) axis through an unknown angle θ. In this coordinate system, the thermal conductivity tensor of the orthotropic sample can be written as

$$\Lambda_{2Oxyz} = \begin{bmatrix} \lambda_{2xx} & \lambda_{2xy} & 0 \\ \lambda_{2xy} & \lambda_{2yy} & 0 \\ 0 & 0 & \lambda_{2zz} \end{bmatrix} \qquad (1)$$

The identification is achieved through the estimation of these four parameters. From them, it is possible to determine the angle θ, that is to say the main directions, as well as the three thermal conductivities along the main axes. To perform the estimation, an inverse method is used. The direct problem is solved using a 3-D finite element solver. The identification of the unknown composite thermal properties is based on the minimisation of a function representing the sum of the differences between the measured temperatures and the calculated temperatures at the same locations.

2.4. Model equations

2.4.1. Spatial domain

The total thickness of the heater is $e_1 = 0{,}5.10^{-3}$ *m*, and its radius is $r_{max} = 120mm$. The mid-plane (*O,x,y,z=0*) of the heater is also a symmetry plane of the assembly. The thickness composite sample e_2 is large enough to consider the composite sample as homogeneous and orthotropic material. The spatial domain Ω of the model equations involves two sub-fields: Ω_1 for the heater and Ω_2 for the composite sample, thus it is described by the elementary cell shown in (fig. 2).

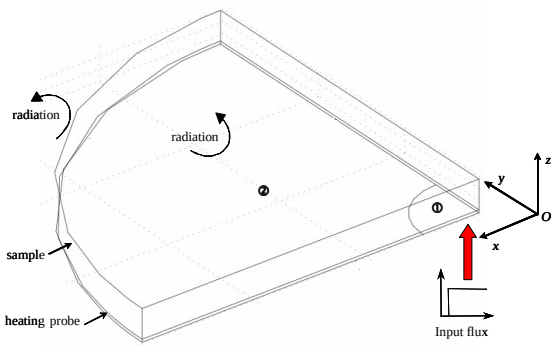

Figure 2: Eighth of the global geometry

2.4.2. Temperature field

At the initial time of the experiment, the temperature of the composite samples and of the heater are uniform and equal to that of the vacuum chamber, so $T(x,y,z,t=0)=T_\infty$ in Ω. The heater is off. For $t\in]0,t_f]$ a uniform heat flux is dissipated by the heater. Then, the temperature fields $T_i(x,y,z,t)$, *i=1,2,* are obtained by solving the heat conduction equation in Ω :

$$(x,y,z)\in\Omega_i\,,\,0<t<t_f\ :\ \rho_i Cp_i\frac{\partial T_i}{\partial t}=\nabla\cdot\left(\Lambda_i\nabla T_i\right) \qquad (2)$$

Λ_1 corresponds to the thermal conductivity tensor of the heater. It is defined by a planar thermal conductivity λ_{1xx}, and a transverse one λ_{1zz}. The following boundary and interface conditions are considered for computing the solution:

- on Γ_0, the lower face of the heater: dissipation of a heat source,
- on $\Gamma_{1,lat}$, the lateral face of the heater, ($r=r_{max}$) and on $\Gamma_{2,lat}\cup\Gamma_{2,up}$, the lateral ($r=r_{max}$) and upper ($z=e_1+e_2$,) faces of the composite: radiative condition,
- on Γ_{int}, the internal boundary between the heater and the composite: heat flux condition where a thermal contact resistance is introduced to account for the non-perfect contact between the heater and the samples. It is assumed to be spatially uniform.

- on the other boundaries, adiabatic conditions are considered to account for the symmetry configuration. Note that *n* is the normal vector to the surface.

2.4.3. Sensitivity fields

The sensitivity field to the parameter vector $\beta=\left[\beta_j\right]_{j=1}^m$ in the sub-field Ω_i is defined by:

$$X_{ij}(x,y,z,t;\beta)=\frac{\partial T_i(x,y,z,t)}{\partial\beta_j}\,,\ j=1..m;\ i=1,2 \qquad (3)$$

In practice, the thermal conductivity tensor, the specific heat, the thermal contact resistance between the heater and the samples, and the emissivity of the external surfaces have to be determined and define an unknown parameter vector. The sensitivity fields are obtained by differentiating the model equations with respect to each component of the parameter vector. It is observed that the sensitivity equations are similar to the heat equation, but they involve additional terms, coupled to the model equations. To avoid storing the coupled terms, it is judicious to calculate

simultaneously the whole fields T_i, X_{ij} *(j=1 to m)* by solving a global set of equations. The calculations of sensitivities to the unknown parameters are very important. On the one hand they directly play a role in the inverse algorithm and on the other hand, they were used to develop the heater design (spatial distribution of the power supply, micro-thermocouples locations) and to inform on the identification feasibility.

2.5. Estimation possibilities

By its conception, the heater design offers two distinct heating configurations. The configuration ① consists in powering the central part of the heater. For isotropic samples, the isotherm lines in the heater plane would be circular. However for orthotropic composite materials, these isotherm lines are distorted in ellipses. Thanks to the micro thermocouples located in the heater, the analysis of the different temperature raises for different locations in the heater plane leads to the determination of the planar thermal conductivities: λ_{2xx}, λ_{2yy} and λ_{2xy}. as well as the specific heat. Moreover, thanks to the pyrometer, the temperature evolution measurement of the external surface of the sample, allows us to estimate the transverse thermal conductivity λ_{2ZZ}.
In the configuration ②, both central part and peripheral corona are powered to dissipate a known uniform heat flux on the entire samples faces that are in contact. In that case, the mid-plane (*O,x,y,z=0*) is isothermal, so that the sensitivity to the parameters λ_{2xx}, λ_{2yy} and λ_{2xy} are null.

2.6. Parameter estimation inverse methodology

The method we use to estimate the thermal properties of composite samples is based on the Ordinary Least Square (O.L.S.) estimation technique. Considering *ns* the number of sensors and *nt* the number of sampling times, the output model vector at the sensor locations can be defined by:

$$Y(\beta) = [C] \cdot T(\beta) \text{ with } \dim(Y) = ns \times nt \qquad (4)$$

where $T(\beta)$ is the finite element approximation of the solution of the model equations, and $[C]$ the sensor location matrix. Measurements are assumed to be corrupted only by an uncorrelated, zero mean, Gaussian, additive noise ε and: $\tilde{Y} = [C] \cdot T + \varepsilon$.
The estimation of $\beta = [\beta_j]_{j=1}^{m}$ consists in minimising the O.L.S. criterion:

$$S(\beta) = \sum_{k=1}^{ns \times nt} \left(\tilde{Y} - Y(\beta) \right)^2 \qquad (5)$$

The model solution $Y(\beta)$ being not linear with respect to β, the minimum $\hat{\beta} = \arg\min S(\beta)$ is computed according to the Gauss Newton algorithm. The sensitivity matrix $X_s = [C] \cdot X$, evaluated at the sensors locations, has to be inversed for each iteration of the inverse algorithm. It is therefore obvious that parameters can be estimated only if sensitivities at the measurement points are linearly independent. Correlation between two parameter components (β_i, β_j) is given by:

$$C(\beta_i, \beta_j) = \frac{\operatorname{cov}(\beta_i, \beta_j)}{\sqrt{\operatorname{var}(\beta_i) \operatorname{var}(\beta_j)}} \qquad (6)$$

$$\text{with } \operatorname{cov}(\beta) = \sigma_N^2 \left(\left(X_s^* \right)^t X_s^* \right)^{-1} \qquad (7)$$

It is also usual to introduce the final relative estimation errors, on each component

$$re(\beta_j) = \sigma_{\beta_j} / \beta_j = \sigma_N \sqrt{Var(\beta_j)} / \beta_j \qquad (8)$$

σ_N is the standard deviation of the measurement noise. It is evaluated during a short period prior to heating. $\sigma_{\beta j}$ is the standard deviation of the estimation error of β_j. The iterative process is stopped when the norm of the residual $\left\|\tilde{Y} - Y(\hat{\beta})\right\|$ is of the same order of magnitude than the measurement noise.

2.7. Experimental results

In order to test the experimental device, the estimation procedure was applied on PMMA and composite samples. PMMA (5.2mm thick) has been selected since its thermal conductivity is low and its thermal properties are well known. External samples faces were painted with a black paint of know emissivity (ε = 0,97).

PMMA samples were instrumented with K-type thermocouples of 80µm. Such instrumentation permits to detect if the heat flux dissipated by the heater is divided in two equal parts in both samples. The estimation of the thermal properties of the PMMA material was realized using the only heating configuration ① since it is an isotropic material. The obtained results (table 1) are closed to the one found in literature and to the one measured by other experimental device.

	Results	Other devices	Literature (T = 20°C) [8]
λ (W/mK)	0.21	0.20	0.193
Cp (J/kg.K)	1502	1532	1380

Table 1: Comparison of PMMA experimental results vs literature, T = 45°C.

The tested material is pure unidirectional composite is an AS4/8552 RC34 AW196 UD tape from Hexcel Composites. The resin content in weight is about 34%, and its density is 1590 kg/m^3. In order to estimate the three components of the thermal conductivity tensor Λ_{2OXYZ}, the angle θ that defines the orientation of the composite main directions in the heater coordinate system and the specific heat, we used both configurations. For the presented results, unidirectional composite samples are oriented so that the fibres direction makes an angle of 20° with the Ox direction of the heater. Temperature responses were analysed using described inverse technique. The results (table 2) are in agreement with other measurements made on this material.

	Results	Other device n°1		Other device n°2	
Temperature:	45°	25°	60°	40°	60°
λ_{2xx} (W/mK)	5.3	5.2	5.7	4.96	5.26
λ_{2yy} (W/mK)	0.69	0.69	0.71	-	-
λ_{2zz} (W/mK)	0.62	-	-	0.68	0.72
Cp (J/kg.K)	1050	983	1043	992	1072

Table 2: Experimental results on unidirectional composite material along the main directions and comparison with other devices measurements.

For the orientation of the main directions, we found θ = 23°, which is close to the expected orientation of the composite fibres (i.e. 20° with respect to (Ox) axis).

3. PREDICTION OF EFFECTIVE THERMAL PROPERTIES FROM MICROSTRUCTURE

In this work, we focused our interest on the prediction of effective thermal conductivities of unidirectional CFRP from the thermal properties of its constituents and the fibres arrangement. Before assuming periodic or random fibres distribution, the microstructure has to be studied. This is achieved through the acquisition of large non-

overlapping composite microstructure images (using mosaïcking technique), the use of post-processing tools (Hough transform, morphological operations from AnalySIS® software) as fibres detection and the calculation of relevant spatial descriptors. Fibres distribution can be then fully characterized and random or anisotropic aspects of the microstructure can be evaluated.
From these results, predictive models of thermal properties based on the RVE of actual composite microstructure were developed.

3.1. A non-random fibres distribution

To get reliable evidence of potential difference between random and CFRP microstructures (figure 3), a material with hard-core random distribution of fibres was computed with the same fibres radii distribution and the same fibres volume fraction (55%) as those measured on experimental micrographs. Several spatial descriptors are then calculated for both type of microstructure.

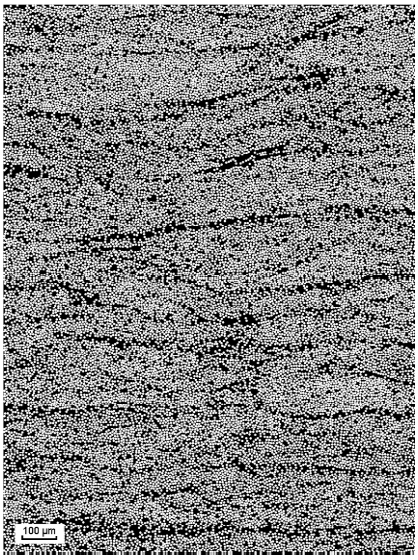

Figure 3: Micrograph of the studied unidirectional CFRP material (fibres are in white).

Dirichlet tessellation of a micrograph into Voronoï cells is useful to quantitatively characterize the microstructure. It identifies the heterogeneities through a 2D cartography and the distribution of the local fibre area fraction ($A_{loc} = S_{fibre} / S_{cell}$), as displayed in figure 4a.

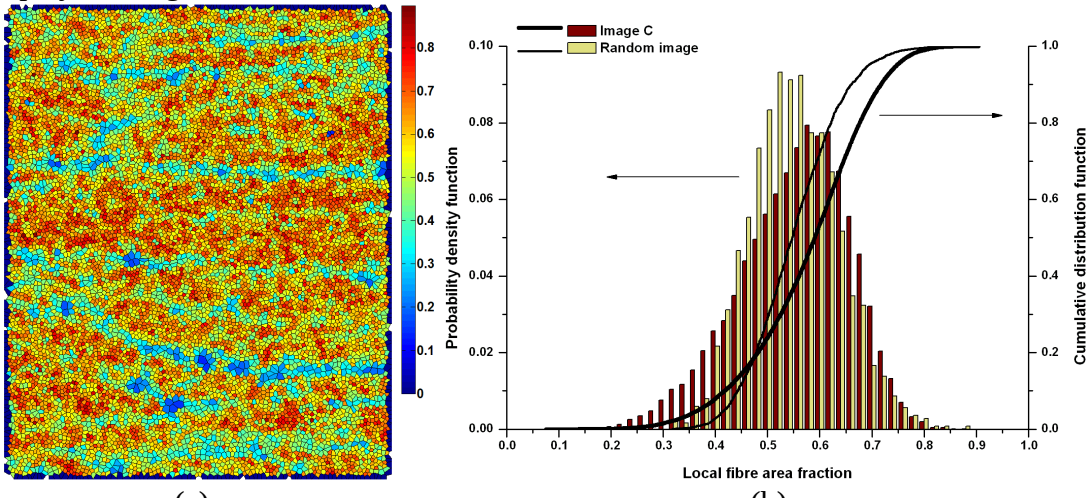

(a) (b)

Figure 4: (a) Voronoï diagram. (b) Cumulative and the probability density functions.

Voronoï diagram of the studied CFRP clearly illustrates that fibres are not uniformly distributed. The color scale brings to light several fibres-rich region (red) split by fibres-poor region (blue) and aligned along the horizontal direction. The fibres-rich bands correspond to the prepreg plies. Dirichlet tessellation of random microstructure does not exhibit such heterogeneity of the local fibre area fraction cartography. The analysis of the associated distributions is useful to quantify the discrepancy. Figure 4b presents the cumulative and the probability density functions ($F(A_{loc})$ and $f(A_{loc})$, respectively) for both microstructures. Regarding the probability density function, a wider dispersion of the local area fraction is observed for the real microstructure. For instance, its $f(A_{loc})$ histogram exhibits a tail at low area fraction, corresponding to the cells located in and near the epoxy-rich regions. This characteristic is reflected on $F(A_{loc})$ by an earlier increase. Moreover, in the [60% - 80%] local area fraction range, the intensity of $f(A_{loc})$ is higher compared to those calculated for the random microstructure. It is attributed to the fact that fibres are tightly packed in the plies.
Other relevant descriptors such as continuous wavelet transform (multi-scale detection) and isotropic and directional pair correlation functions were also computed from random and composite microstructures. All these parameters also demonstrate a deviation of the CFRP material from random fibres distribution. It is then of paramount importance to take this peculiar microstructure into account for thermal properties calculation.

3.2. Anisotropic character of CFRP microstructure

Since the fibres distribution of the CFRP is not random, one can wonder if fibres are located along preferential directions, indicating anisotropy. However, spatial descriptors sensitive to the analysis direction are not numerous. The covariance function is suitable to underline the geometrical dispersion of a two-phase system since the covariance is a signature of the size and arrangements of objects. From the analysis of the rose of directions computed from composite micrograph, we identified two preferential orientations: parallel and perpendicularly to the plies. Therefore, the covariance function $C_\alpha(h)$ is calculated for these two directions. It is plotted in figure 5. For h=0, the value of $C_\alpha(h)$ is, as expected, equal to 55.2%, which the exact area fraction of the studied micrograph. The locations of the first nearest neighbours are the same in both directions up to the fourth peak.

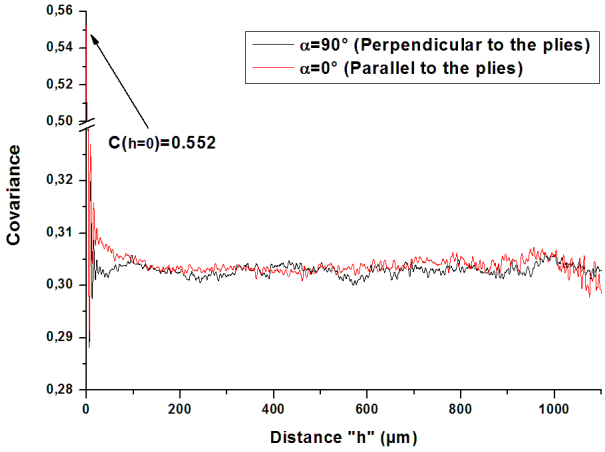

Figure 5: Covariance function calculated for preferential orientations

Beyond, the peaks are less defined. The curves exhibit significant variations according to the studied direction (α=0° or 90°). $C_{90°}(h)$ decreases more rapidly to the asymptotic value than $C_{0°}(h)$. This is clearly induced by the plies / inter-plies arrangement: because

of inter-plies, the correlation between the fibres drops rapidly rather than along plies direction where less local fibres density variations are found. On can also notice on $C_{90°}(h)$ weak oscillations of wider wavelength getting a period of 180 µm. It is due to the inter-plies since this length is the order of magnitude of one ply thickness. However, variations of plies thicknesses induce non-regular broad oscillations of $C_{90°}(h)$.

Thanks to covariance results, we conclude that the microstructure exhibit anisotropic properties. However, it seems that this anisotropy is weak since the differences observed along the two main directions have a small intensity. Nevertheless it does not induce a weak anisotropy of thermal properties because other parameters as thermal contrast are very influent. This point is discussed in the next section.

3.3. RVE and prediction of effective thermal conductivities

The models provide effective properties on condition that computations are performed on a representative area of the whole composite. The determination of the RVE is therefore a crucial point of interest. A unique RVE does not exist. It is generally different from one property to another. From a microstructural point of view, RVEs were determined from fibre area fraction (V_f), isotropic and directional pair correlation functions (named g(r) and $g_\alpha(r)$). If no RVE can be found at the ply scale, two different RVE sizes (L×L square windows) are defined according the considered spatial descriptors; L=612 µm for V_f and $g_\alpha(r)$ and L= 412 µm for g(r).

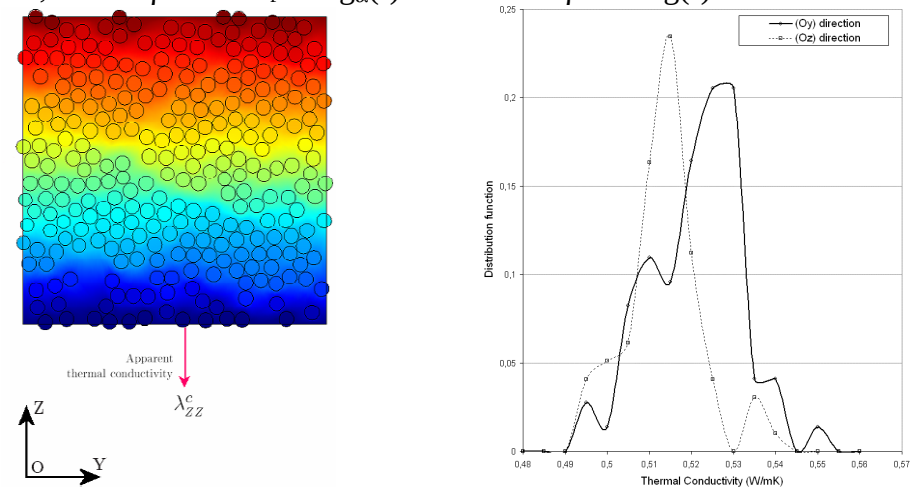

(a) (b)

Figure 6: (a) Calculation of thermal response of microstructure from the Unit Cell method. (b) Distribution of thermal conductivities along (OZ) and (OY)

A classical way to determine thermal properties of heterogeneous materials is the Unit Cell method. It permits to calculate the apparent thermal conductivity of a window containing extract of composite microstructure; an unitary thermal gradient is imposed and thermal response is computed (figure 6a). The resulting heat is integrated on the boundaries ($<\phi(z)>$) so as to estimate the apparent transverse thermal conductivity ($\lambda_{zz}=L\times<\phi(z)>$). In this work, Finite Element is used to solve thermal problem. Thermal conductivity of resin is λ_r=0.22 W/m.K and the radial thermal conductivity of carbon fibre is λ_f=1.19 W/m.K. Admitting its existence, the RVE size is estimated performing a analysis of the results dispersion for each window size: below a relative error of 1% (fixed by experimenter) the RVE is considered to be reached. For the studied composite, we observed both curves are below a 1% value when the window size reaches L ≈ 300µm. It is much lower than the one found from morphological

properties. Considering this “thermal RVE”, calculations points out a difference of thermal conductivity (2%) between both directions: λ_{yy}=0.526 W/m.K and λ_{zz} = 0.518 W/m.K. This confirms the weak anisotropy of this material already detected with the microstructural analysis. A stronger thermal anisotropy could be expected but thermal contrast is finally too weak to induce important anisotropy.
An other important advantage of predictive models is the possibility to provide a distribution of thermal conductivity, working on numerous images with a size at least equal to the RVE. Curves are presented in figure 6b. They underline the weak anisotropy and also represent the probability of finding a thermal conductivity for this material.

4. CONCLUSIONS

Thermal characterization of composite materials is performed following two parallel routes. The first one is experimental and consists in designing a new device, which can provides the whole parameters of effective thermal conductivity tensor in the main directions and the specific heat. No instrumentation of sample is required and one experiment can be sufficient to determine of the parameters.
The second approach is the development of predictive models based on composite microstructure. The reliability of the results is linked to its representativeness. Therefore, the RVE is identified. Microstructural characterization is performed on a unidirectional CFRP material. We highlight a non-random fibres distribution and a weak anisotropy. The RVE is estimated to L=612µm from several spatial descriptors. This anisotropy is confirmed with numerical prediction of thermal conductivity, which exhibits a systematic difference between main directions (2%). The associated RVE is lower than the previous one since we find L=300µm. Finally, predictive models permits to get a dispersion of the thermal conductivity results.

ACKNOWLEDGEMENTS

The authors thank Airbus® industry for the financial support of this work.

REFERENCES

1- Grigull U. and Sandner H., “Heat conduction”. Springer Verlag, 1984.
2- Parker, Jenkins, Butler, Abbot, “Flash methods of determining thermal diffusivity, heat capacity and thermal conductivity”, *Journal of Applied Physics*, 1961;23:1679-l684.
3- Degiovanni A., Batsale J.C., Maillet D., “Mesure de la diffusivité longitudinale de matériaux anisotropes”, *Revue Générale de Thermique*, 1996;35:141-147.
4- Pyrz R, Bochenek B., “Topological disorder of microstructure and its relation to the stress field”, *International Journal of Solids Structures*, 1998;35(19):2413-2427.
5- Shan Z, Gokhale A M., “Representative volume element for non-uniform microstructure”, *Computational in Material Science*, 2002;24:361-379.
6- Kanit T, Forest S, Galliet I, Mounoury V, Jeulin D., “Determination of the size of the representative volume element for random composites: statistical and numerical approach”, *International Journal of Solids Structures*, 2003;40:3647-3679.
7- Coindreau O, Vignoles G., “Computing structural and transport properties of C/C composites from 3D tomographic images”, *Material Science Forum*, 2004; 455-456: 751-754.
8- D.W. Van Krevelen, Properties of polymers, Elsevier, Amsterdam, 1990.